Journal of Zhejiang University-SCIENCE B (Biomedicine & Biotechnology) *2023 24(1):64-77*
www.jzus.zju.edu.cn; www.springer.com/journal/11585
E-mail: jzus_b@zju.edu.cn

Research Article

https://doi.org/10.1631/jzus.B2200272

A novel defined risk signature of endoplasmic reticulum stress-related genes for predicting the prognosis and immune infiltration status of ovarian cancer

Jiahang MO[1,2*], Shunyi RUAN[3*], Baicai YANG[4], Yunfeng JIN[1,2], Keyi LIU[5], Xukai LUO[1], Hua JIANG[1,2✉]

[1]*Obstetrics and Gynecology Hospital, Fudan University, Shanghai 200011, China*
[2]*Shanghai Key Laboratory of Female Reproductive Endocrine Related Diseases, Obstetrics and Gynecology Hospital, Fudan University, Shanghai 200011, China*
[3]*Department of Oncology, Shanghai Sixth People's Hospital Affiliated to Shanghai Jiao Tong University School of Medicine, Shanghai 200233, China*
[4]*Department of Gynecology, Jiaxing University Affiliated Women and Children Hospital, Jiaxing 314050, China*
[5]*Department of Pathology, Women's Hospital, School of Medicine, Zhejiang University, Hangzhou 310006, China*

Abstract: Endoplasmic reticulum (ER) stress, as an emerging hallmark feature of cancer, has a considerable impact on cell proliferation, metastasis, invasion, and chemotherapy resistance. Ovarian cancer (OvCa) is one of the leading causes of cancer-related mortality across the world due to the late stage of disease at diagnosis. Studies have explored the influence of ER stress on OvCa in recent years, while the predictive role of ER stress-related genes in OvCa prognosis remains unexplored. Here, we enrolled 552 cases of ER stress-related genes involved in OvCa from The Cancer Genome Atlas (TCGA) and Gene Expression Omnibus (GEO) cohorts for the screening of prognosis-related genes. The least absolute shrinkage and selection operator (LASSO) regression was applied to establish an ER stress-related risk signature based on the TCGA cohort. A seven-gene signature revealed a favorable predictive efficacy for the TCGA, International Cancer Genome Consortium (ICGC), and another GEO cohort (P<0.001, P<0.001, and P=0.04, respectively). Moreover, functional annotation indicated that this signature was enriched in cellular response and senescence, cytokines interaction, as well as multiple immune-associated terms. The immune infiltration profiles further delineated an immunologic unresponsive status in the high-risk group. In conclusion, ER stress-related genes are vital factors predicting the prognosis of OvCa, and possess great application potential in the clinic.

Key words: Ovarian cancer (OvCa); Endoplasmic reticulum (ER) stress; Risk signature; Prognosis; Immune infiltration

1 Introduction

Ovarian cancer (OvCa) is the most lethal malignancy occurring in the female reproductive system, globally ranked as the eighth leading cause of female cancer-related deaths (Sung et al., 2021; Tian et al., 2022). According to the global cancer statistics, the number of new OvCa cases reached 313 959 in 2020 with 207 252 deaths (Sung et al., 2021). Therapeutic advancements, including the application of targeted drugs, such as poly adenosine diphosphate (ADP)-ribose polymerase (PARP) inhibitors (González-Martín et al., 2019; Poveda et al., 2021) or anti-angiogenesis agents (Pujade-Lauraine et al., 2014), and reinspection of secondary cytoreduction (Harter et al., 2021), have improved the outcomes of OvCa patients to some extent, with an overall five-year survival rate of 47% (Lheureux et al., 2019). In this scenario, prognosis prediction is crucial for patients to obtain meaningful treatment, but is hindered by the high heterogeneity of OvCa. Strikingly, numerous risk models, including the ferroptosis-based (Ye et al., 2021), autophagy-based (Fei et al., 2021), and immune-related (Zhang B et al., 2021) approaches, have been developed to predict OvCa patients' prognosis along with the application of bioinformatics. Despite that commonalities may be

✉ Hua JIANG, jianghua_fckyy@126.com
* The two authors contributed equally to this work
Jiahang MO, https://orcid.org/0000-0002-2418-1745
Shunyi RUAN, https://orcid.org/0000-0003-0974-4463
Hua JIANG, https://orcid.org/0000-0002-5235-341X

Received May 9, 2022; Revision accepted Aug. 30, 2022; Crosschecked Jan. 11, 2023

present, the gene signatures derived from the variety of phenotypes highlight the different aspects of disease. Thus, novel gene signatures based on the core processes of cell fate and interaction with the surroundings need to be constantly explored to improve the accessibility of prognostic prediction for OvCa.

Protein handling, modification, and assembly in the endoplasmic reticulum (ER) are tightly regulated processes that determine cell function and fate (Chen and Cubillos-Ruiz, 2021). ER stress occurs when mammalian cells encounter exogenous cell stress, such as hypoxia, nutrient deprivation, and the accumulation of reactive oxygen species (ROS), causing a burden of misfolded proteins in the ER lumen (Andrews et al., 2021). Three sensors that detect ER stress, including inositol-requiring enzyme 1α (IRE1α)/X-box-binding protein 1 (XBP1), protein kinase RNA-like ER kinase (PERK), and activating transcription factor 6 (ATF6), then ensue to restore homeostasis (Cubillos-Ruiz et al., 2016). Meanwhile, under the unremitting stress, cells are inclined to undergo apoptosis through effector proteins such as CCAAT/enhancer binding protein (C/EBP)-homologous protein (CHOP) (Lin et al., 2021). The critical role of ER stress orchestrating adaptive programs to modulate cancer cell fate has recently been highlighted in the realm of OvCa research. By targeting the IRE1α/XBP1 pathway, Lin et al. (2021) found that B-I09, an IRE1α inhibitor, can suppress the growth of OvCa cells with certain mutations in vitro and in xenograft models. Surprisingly, the IRE1α/XBP1 pathway was also involved in the regulation of OvCa stemness according to an eminent work by Zhang et al. (2022). A newly defined stem-related transcription factor (TF), forkhead box K2 (FOXK2), directly upregulates the IRE1α expression, leading to the formation of XBP1 and the initiation of stemness pathways (Zhang et al., 2022). In contrast, activation of PERK branch together with the ATF4-mediated transcriptional induction of CHOP is greatly regarded as a symbol of pro-apoptosis. A study conducted by Lee et al. (2020) ascertained the pro-apoptotic role of PERK arm, in which the application of apomorphine induced mitochondrion-associated apoptosis and triggered ER stress accompanied by phosphorylation of PERK in OvCa. However, the role of ATF6 arm in OvCa remains to be explored.

The ER stress-related apoptosis is deemed to be a kind of immunogenic cell death (ICD), which is characterized by the exposure of damage-associated molecular patterns (DAMPs), such as calreticulin (CRT) and heat shock proteins (HSPs) (Galluzzi et al., 2017). Studies have indicated that CRT exposure was able to provide a robust innate and adaptive antitumor immune response, leading to favorable prognosis in OvCa patients (Kasikova et al., 2019). The tumor microenvironment (TME) is replete with factors that cause stress to intratumoral immune cells (Andrews et al., 2021); thus, the ER stress pathway is also implicated in infiltrating immune cells (Lin et al., 2021). Unlike its pro-survival role in OvCa cells, IRE1α/XBP1 arm activation in dendritic cells (DCs) impaired the function of antigen presentation under the OvCa milieu, further driving disease progression (Cubillos-Ruiz et al., 2015). Based on these findings, investigations are necessary to ascertain the ambiguous role of ER stress in the TME.

In this study, we enrolled 552 cases of OvCa-involved ER stress-related genes from two datasets to form a seven-gene risk signature. By employing two external cohorts, we validated the accuracy and credibility of our model, and ascertained that the gene signature was an independent predictive factor for OvCa patients. Overall, our study successfully constructed an ER stress-related risk model that can be potentially applied in the clinic.

2 Results

2.1 Development of a risk model using seven identified ER stress-related genes

We identified the prognosis-related genes from The Cancer Genome Atlas (TCGA)-ovarian cancer (OV) cohort (n=368) and the Gene Expression Omnibus (GEO) dataset (accession number: GSE26712; n=184) by univariate Cox regression analyses (Tables S1 and S2). The gene numbers were shown in the workflow diagram (Fig. 1a). After intersection, eight possible prognosis-related genes were screened out (P<0.05), namely, transient receptor potential cation channel subfamily V member 4 (*TRPV4*), insulin-like growth factor 2 receptor (*IGF2R*), forkhead box O1 (*FOXO1*; absent in GSE49997 dataset), retinoblastoma 1 (*RB1*) gene, heat shock protein (HSP) family A (HSP70) member 2 (*HSPA2*), paxillin (*PXN*), transporter 1 adenosine triphosphate (ATP)-binding cassette subfamily B

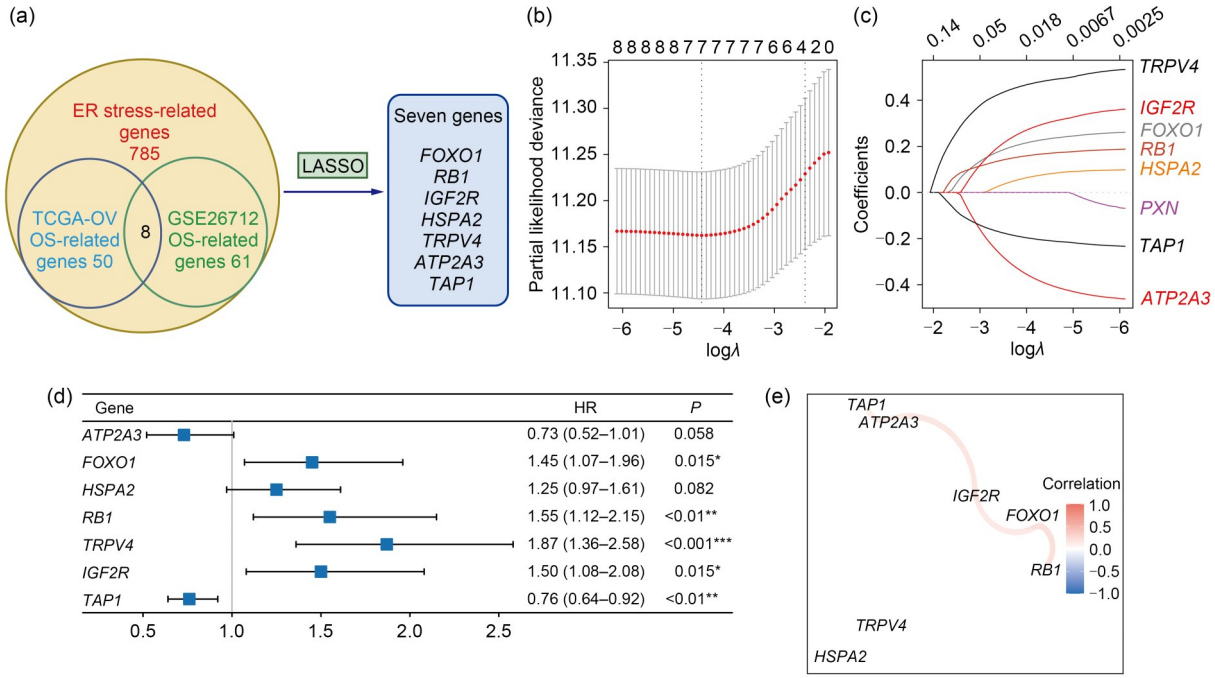

Fig. 1 Identification of prognostic genes for developing a risk signature. (a) Workflow diagram of seven genes screening. (b) Selection of the optimal parameter (λ) in the LASSO model. (c) LASSO coefficient profiles of the eight genes in TCGA cohort. (d) Establishment of a prognosis signature by seven chosen genes. * P<0.05, ** P<0.01, *** P<0.001. (e) The correlation network of the seven genes. ER: endoplasmic reticulum; TCGA: The Cancer Genome Atlas; OS: overall survival; LASSO: least absolute shrinkage and selection operator; *FOXO1*: forkhead box O1; *RB1*: retinoblastoma 1; *IGF2R*: insulin-like growth factor 2 receptor; *HSPA2*: heat shock protein family A member 2; *TRPV4*: transient receptor potential cation channel subfamily V member 4; *ATP2A3*: ATPase sarcoplasmic/endoplasmic reticulum Ca^{2+} transporting 3; *TAP1*: transporter 1 adenosine triphosphate (ATP)-binding cassette subfamily B member; *PXN*: paxillin; HR: hazard ratio.

member (*TAP1*), and ATPase sarcoplasmic/endoplasmic reticulum Ca^{2+} transporting 3 (*ATP2A3*). The least absolute shrinkage and selection operator (LASSO) regression analysis was then performed to select the most robust prognostic genes from the eight ER stress-related genes. Finally, seven of the eight genes and their coefficients were retained according to the optimal λ value decided by the minimum criteria (Figs. 1b and 1c). Among these genes, *ATP2A3* and *TAP1* were protective factors for OvCa survival, with hazard ratio (HR)<1; while *FOXO1*, *HSPA2*, *RB1*, *TRPV4*, and *IGF2R* were risk factors with HR>1 (Fig. 1d). A correlation network based on the expression profiles of seven genes was constructed to identify the relationships among them (Fig. 1e).

2.2 Development of an ER stress-related risk signature in the TCGA-OV cohort

Given the privilege of sufficient sample size, the TCGA-OV cohort was designated for building the risk signature. The formula for calculating the risk score was as follows: risk score=(−0.3963×*ATP2A3* expression)+(0.2318×*FOXO1* expression)+(0.0795×*HSPA2* expression)+(0.1691×*RB1* expression)+(0.4853×*TRPV4* expression)+(0.3016×*IGF2R* expression)+(−0.2078×*TAP1* expression). According to the median risk score, 184 patients were classified as the low-risk group, while the remaining 184 were classified as the high-risk group (Fig. 2a). Principal component analysis (PCA) and *t*-distributed stochastic neighbor embedding (*t*-SNE) analysis were conducted to assign the patients in these clusters (Figs. S1a and S1b). The overall survival (OS)-related prediction model distribution of patients was illustrated in Fig. 2b, implying that patients in the high-risk group had a higher possibility of death and shorter survival time. The expression level of each ER stress-related signature was obviously changed between the two groups (Fig. 2c). The Kaplan-Meier (K-M) curves showed that patients in the low-risk group had a more favorable survival outcome than those in the high-risk group (P<0.0001; Fig. 2d). Time-dependent receiver operating characteristic (ROC)

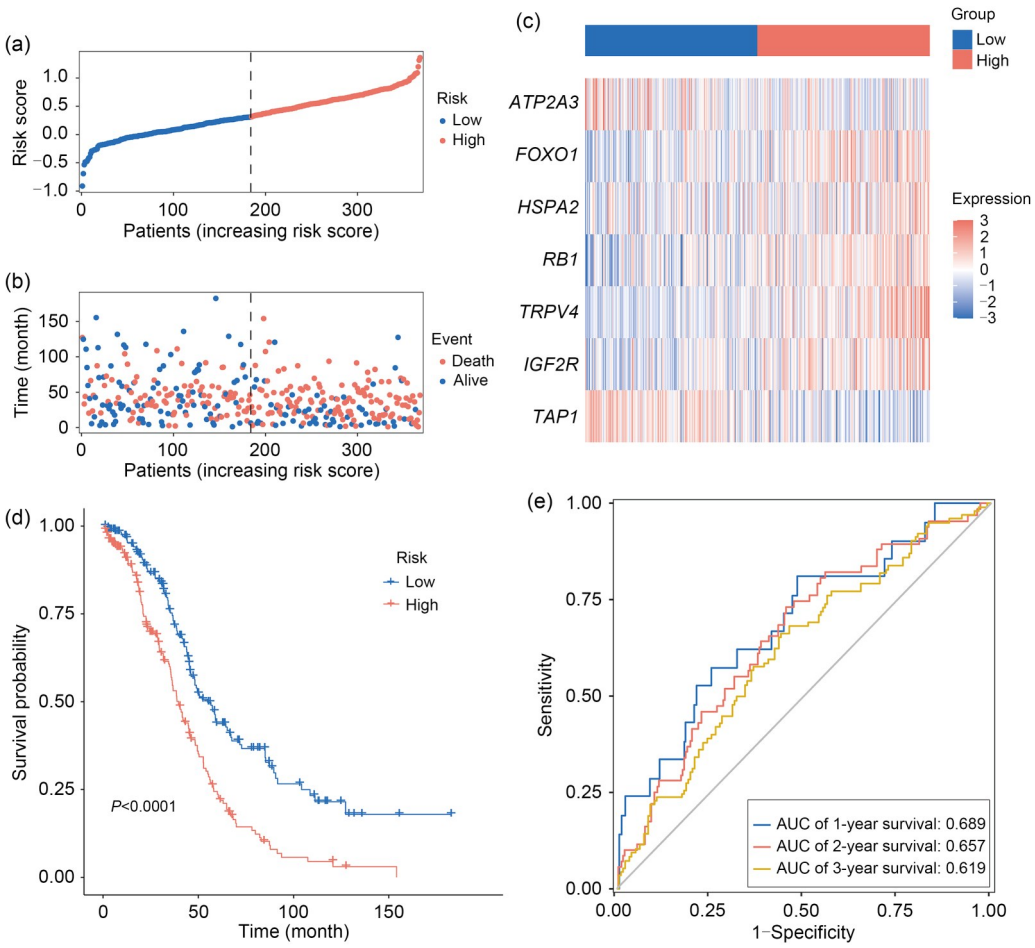

Fig. 2 Training of ER stress-related risk signature for OvCa in TCGA cohort. (a) Risk score for OvCa. (b) Survival status for each case. (c) Heatmap of gene expression between the low- and high-risk groups. (d) K-M curves for the OS of patients in the low- and high-risk groups based on risk score. (e) Time-dependent ROC curve demonstration of the predictive efficiency. ER: endoplasmic reticulum; OvCa: ovarian cancer; TCGA: The Cancer Genome Atlas; K-M: Kaplan-Meier; OS: overall survival; ROC: receiver operating characteristic; *ATP2A3*: ATPase sarcoplasmic/endoplasmic reticulum Ca^{2+} transporting 3; *FOXO1*: forkhead box O1; *HSPA2*: heat shock protein family A member 2; *RB1*: retinoblastoma 1; *TRPV4*: transient receptor potential cation channel subfamily V member 4; *IGF2R*: insulin-like growth factor 2 receptor; *TAP1*: transporter 1 adenosine triphosphate (ATP)-binding cassette subfamily B member; AUC: area under the curve.

curves were conducted for assessing the predictive role of ER stress-related risk signature on OS. As presented in Fig. 2e, the area under the curve (AUC) was 0.689 for one year, 0.657 for two years, and 0.619 for three years. The K-M curves of seven single genes were further extended to validate the predictive value of this signature in the TCGA-OV cohort (Fig. S2).

2.3 Independent prognostic value of ER stress-related risk signature in the TCGA-OV cohort

Univariate and multivariate Cox analyses were subsequently applied to explore whether the risk score could be an independent risk factor in the TCGA-OV training cohort. As illustrated in Figs. 3a and 3b, the ER stress-related risk signature was significantly correlated with the OS of OvCa patients (HR, 2.99; 95% confidence interval (CI), 2.08–4.29; $P<0.001$; refer to multivariate Cox analyses), indicating that the ER stress-related risk signature constructed by the TCGA-OV cohort was an independent prognostic factor for OvCa patients. The multi-indicator ROC curves (Fig. 3c) showed the predictive value of the risk signature and the clinical features, which indicated that the predictive accuracy of the ER stress-related risk model was superior in terms of age, grade, and stage.

Furthermore, a nomogram integrating ER stress risk signature, grade, age, and stage was produced to predict 1-, 3-, and 5-year Os in the TCGA-OV cohort

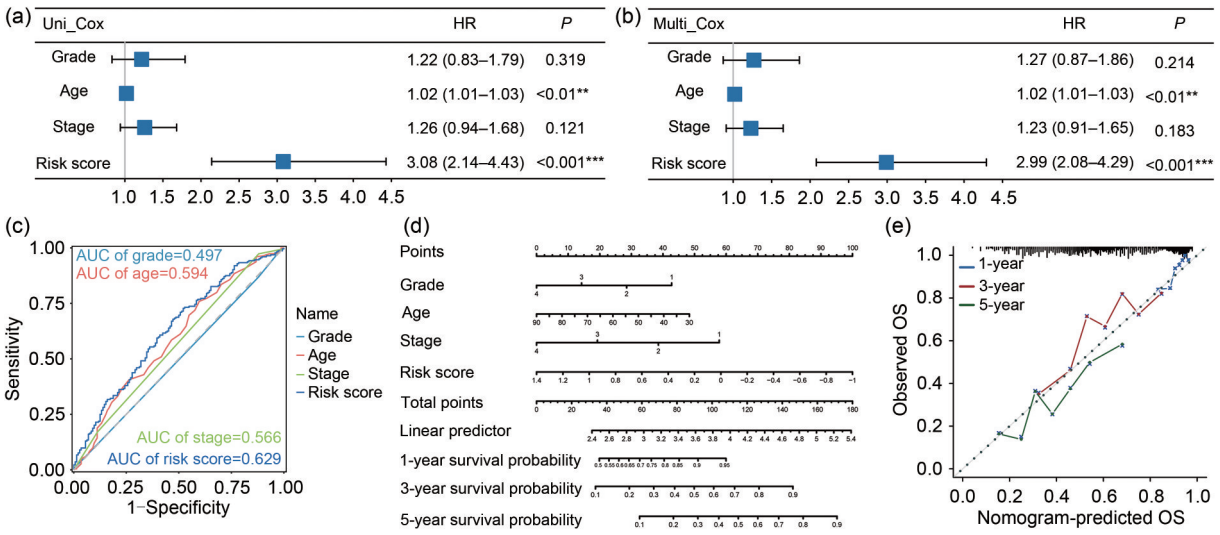

Fig. 3 Independent prognostic value of the ER stress-related risk signature in TCGA cohort. ** ***P*<0.01, *** ***P*<0.001. **(a) Univariate analysis for TCGA cohort. (b) Multivariate analysis for TCGA cohort. (c) Multi-indicator ROC curves for tumor grade, age, stage, and risk score. (d) Nomogram combining seven gene markers in TCGA cohort. (e) The calibration curves for internal verification nomogram in the TCGA cohort. ER: endoplasmic reticulum; TCGA: The Cancer Genome Atlas; ROC: receiver operating characteristic; HR: hazard ratio; AUC: area under the curve; OS: overall survival.**

(Fig. 3d). In the nomogram, each item was assigned to point according to its risk contribution to OS. Calibration curves were used for internal verification of the nomogram (Fig. 3e). Collectively, these data suggested that the ER stress-related risk signature could serve as an independent risk factor in the TCGA-OV cohort.

2.4 Validation of ER stress-related risk signature in the International Cancer Genome Consortium (ICGC) and GEO cohorts

A total of 117 cases from the ICGC and 193 cases from the GEO dataset (accession number: GSE49997) were treated as the external validation sets. Seven or six (*FOXO1* is absent in GSE49997) survival-related genes were extracted from the expression profiling array. The risk score of each sample in the two validation sets was calculated, using the same formula as that in the TCGA-OV cohort. PCA and *t*-SNE analyses were used to visualize the distribution of risk amongst different populations in line with the risk gene sets (Figs. S1c–S1f).

Figs. 4a and 4b showed the OS-related risk model distribution of populations in the ICGC and GEO datasets, respectively. The heatmaps representing the expression level of each risk signature related to ER stress, showed the tendency of changes between the low- and high-risk populations in the validation sets (Figs. 4c and 4d). Interestingly, we further found that the high-risk group had a significantly lower survival possibility than that of the low-risk group in both validation sets (P=0.0032 in ICGC cohort and P=0.04 in GSE49997 cohort; Figs. 4e and 4f). And then, time-dependent ROC curves were drawn to evaluate the predictive value of ER stress-related risk signature in the validation sets. As shown in Figs. 4g and 4h, the AUC was 0.623 for two years and three years in the ICGC cohort, and it was 0.673 for one year, 0.654 for two years, and 0.612 for three years in the GSE49997 cohort, indicating the robust predictive role of our model in the validation cohorts. The forest plots of univariate and multivariate Cox analyses were applied again for the purpose of identifying the independent prognostic role of our risk model (Figs. S1g and S1h). Nomograms integrated by ER stress risk signature and accessible clinical parameters were also constructed to predict the OS in both validation cohorts (Figs. S1i and S1j). Calibration curves were used for internal verification of the nomogram (Figs. S1k and S1l). The above data tested in two external cohorts demonstrated the robustness of this risk model.

2.5 Correlation of the risk signature with canonical ER stress pathways and its functional annotation

Three canonical ER stress pathways have been previously identified that may determine the cell fate through different orientations. The correlation between

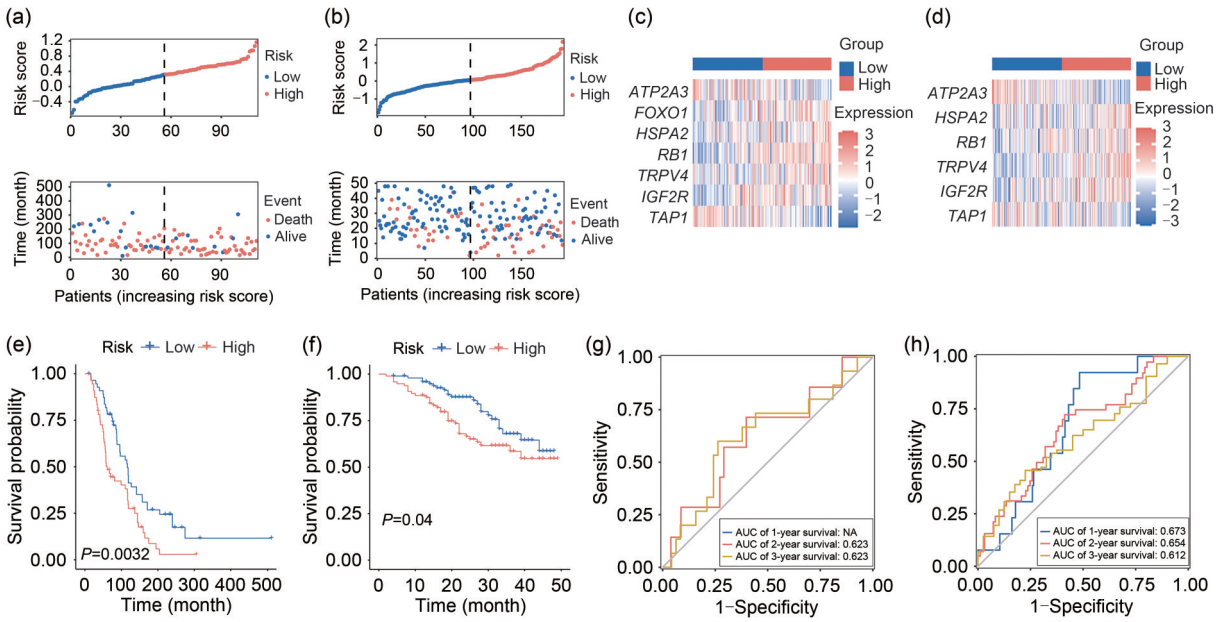

Fig. 4 Validation of ER stress-related risk signature in ICGC and GEO cohorts. (a) Risk score (upper) and distribution of survival status (lower) for OvCa in ICGC cohort. (b) Risk score (upper) and distribution of survival status (lower) for OvCa in GEO cohort. Heatmaps of gene expression between low- and high-risk groups in ICGC (c) and GEO (d) cohorts. K-M curves for the OS of patients between low- and high-risk groups in ICGC (e) and GEO (f) cohorts. Time-dependent ROC curves for OvCa in ICGC (g) and GEO (h) cohorts. *P*<0.05 were considered statistically significant. ER: endoplasmic reticulum; ICGC: International Cancer Genome Consortium; GEO: Gene Expression Omnibus; OvCa: ovarian cancer; K-M: Kaplan-Meier; OS: overall survival; ROC: receiver operating characteristic; *ATP2A3*: ATPase sarcoplasmic/endoplasmic reticulum Ca^{2+} transporting 3; *FOXO1*: forkhead box O1; *HSPA2*: heat shock protein family A member 2; *RB1*: retinoblastoma 1; *TRPV4*: transient receptor potential cation channel subfamily V member 4; *IGF2R*: insulin-like growth factor 2 receptor; *TAP1*: transporter 1 adenosine triphosphate (ATP)-binding cassette subfamily B member; AUC: area under the curve; NA: not available.

our risk signature and the hub genes of these canonical ER stress pathways was analyzed to identify ER stress status in different OvCa groups. In the high-risk group, the levels of IRE1α and PERK were higher than those in the low-risk group, though with a smaller statistical significance in the GSE49997 dataset. Interestingly, the pro-apoptosis arm (*ATF4* and *CHOP*) was upregulated in the low-risk group, demonstrating the cell fate-related role of our signature (Figs. 5a–5c). To estimate the function of these prognosis-related genes, Gene Ontology (GO) and Kyoto Encyclopedia of Genes and Genomes (KEGG) pathway analyses were performed. The top five enrichment terms of GO are shown in Fig. 5d, and the top four enrichments of KEGG are shown in Fig. 5e. The gene set enrichment analysis (GSEA) approach was further employed to replenish the function annotation of these genes. The results demonstrated that these genes were enriched in multiple cytokines interaction and immune-associated terms (Fig. S3).

2.6 Immune infiltrating profiles of ER stress-related risk signature

Considering the accumulating evidence that immune cells infiltrated into the OvCa environment play a pivotal role in disease progression, a heatmap was performed to display the distribution profile of immune cells of each case in the TCGA-OV cohort according to the risk score (Fig. 6a). The CIBERSORT algorithm was further applied to clarify the correlation between ER stress-related risk signature and immune infiltration. Fig. 6b revealed that the fraction of immune cells varied among the cases and groups; Fig. 6c presented the significant differences of immune cell infiltration between the low- and high-risk groups. For the innate immunity cluster, the proportions of dendritic cells (DCs), M1 macrophages, and activated natural killer (NK) cells were significantly decreased in the high-risk group; conversely, the proportions of M0 macrophages, M2 macrophages, activated mast cells, and neutrophils were elevated in the high-risk group. For

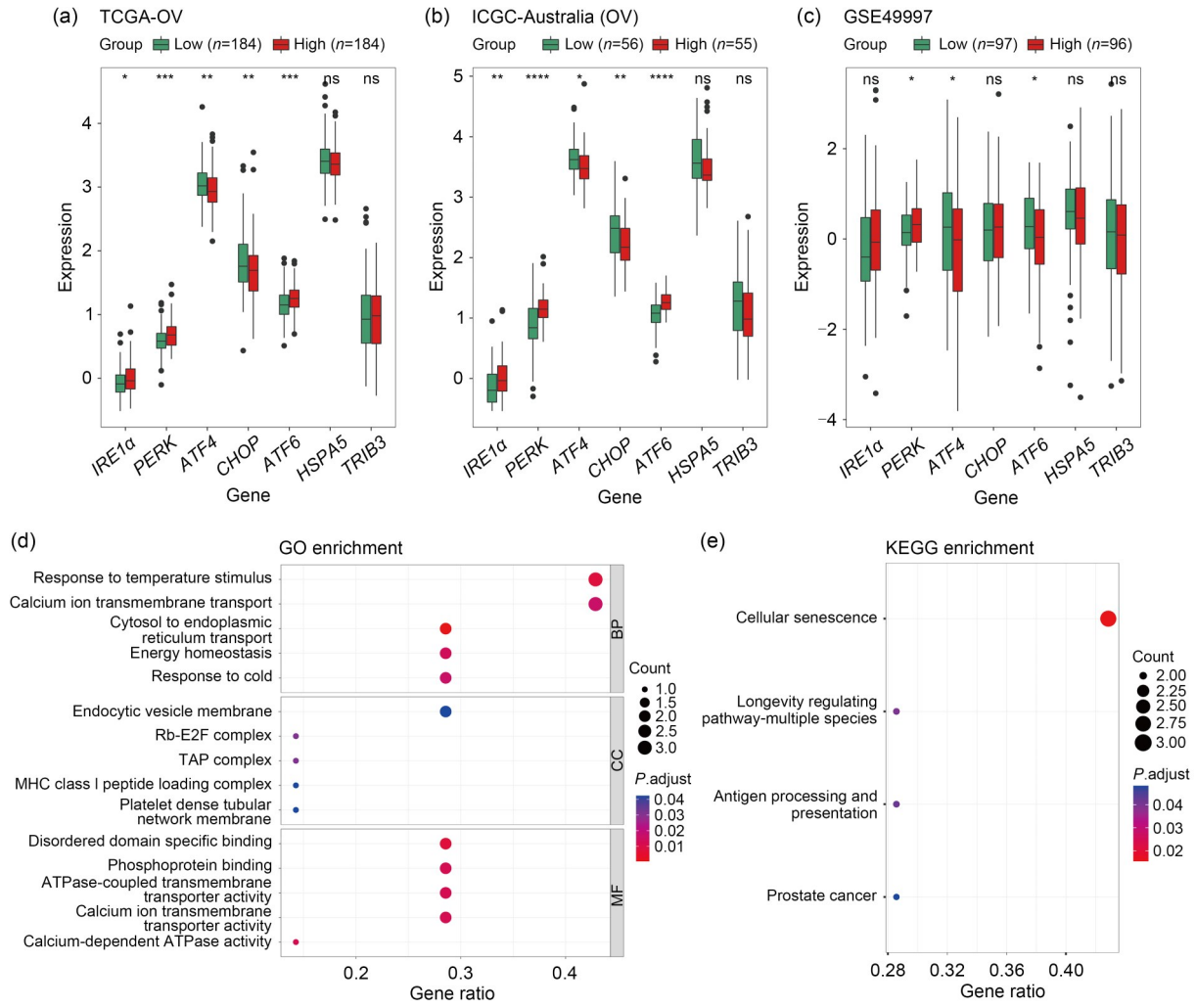

Fig. 5 Functional enrichment of the ER stress-related risk signature. Differential expression of ER stress markers in TCGA (a), ICGC (b), and GEO (c) cohorts between different groups. (d) Bubble graph for GO enrichment. (e) Bubble graph for KEGG pathway. * *P*<0.05, ** *P*<0.01, * *P*<0.001, **** *P*<0.0001, ns: no significance. ER: endoplasmic reticulum; TCGA: The Cancer Genome Atlas; ICGC: International Cancer Genome Consortium; GEO: Gene Expression Omnibus; OV: ovarian cancer; GO: Gene Ontology; KEGG: Kyoto Encyclopedia of Genes and Genomes; BP: biological process; CC: cell component; MF: molecular function; *IRE1α*: inositol-requiring enzyme 1α; *PERK*: protein kinase RNA-like ER kinase; *ATF4*: activating transcription factor 4; *CHOP*: CCAAT/enhancer binding protein (C/EBP)-homologous protein; *HSPA5*: heat shock protein family A member 5; *TRIB3*: tribbles pseudokinase 3; Rb: retinoblastoma; E2F: retinoblastoma-binding protein 3; TAP: transporter associated with antigen processing; MHC: major histocompatibility complex; ATPase: adenosine triphosphatase.**

the other part of the immune system, that is, the adaptive immunity, there were lower gatherings of memory B cells, activated memory cluster of differentiation 4-positive ($CD4^+$) T cells, $CD8^+$ T cells, and follicular helper T cells (Tfh) in the high-risk group, which indicated a potentially decreased anti-tumor efficiency. The immune-related molecules expressed in the OvCa milieu were subsequently analyzed. As shown in Fig. 6d, the expression levels of both immune-activated and immunosuppressive molecules were declined in the high-risk group vs. the low-risk group. Interestingly, among the seven genes, *TAP1* was identified as the most typical player related to immune function, which was implicated in the assembly of antigen peptide-major histocompatibility complex-I (pMHC-I) (Han et al., 2008). Given the knowledge that the activation of $CD8^+$ T cells relies on the recognition of pMHC-I, correlation analysis was conducted in three cohorts (Figs. 6e–6g). The expression level of *TAP1* was significantly positively correlated with *CD8*, which might

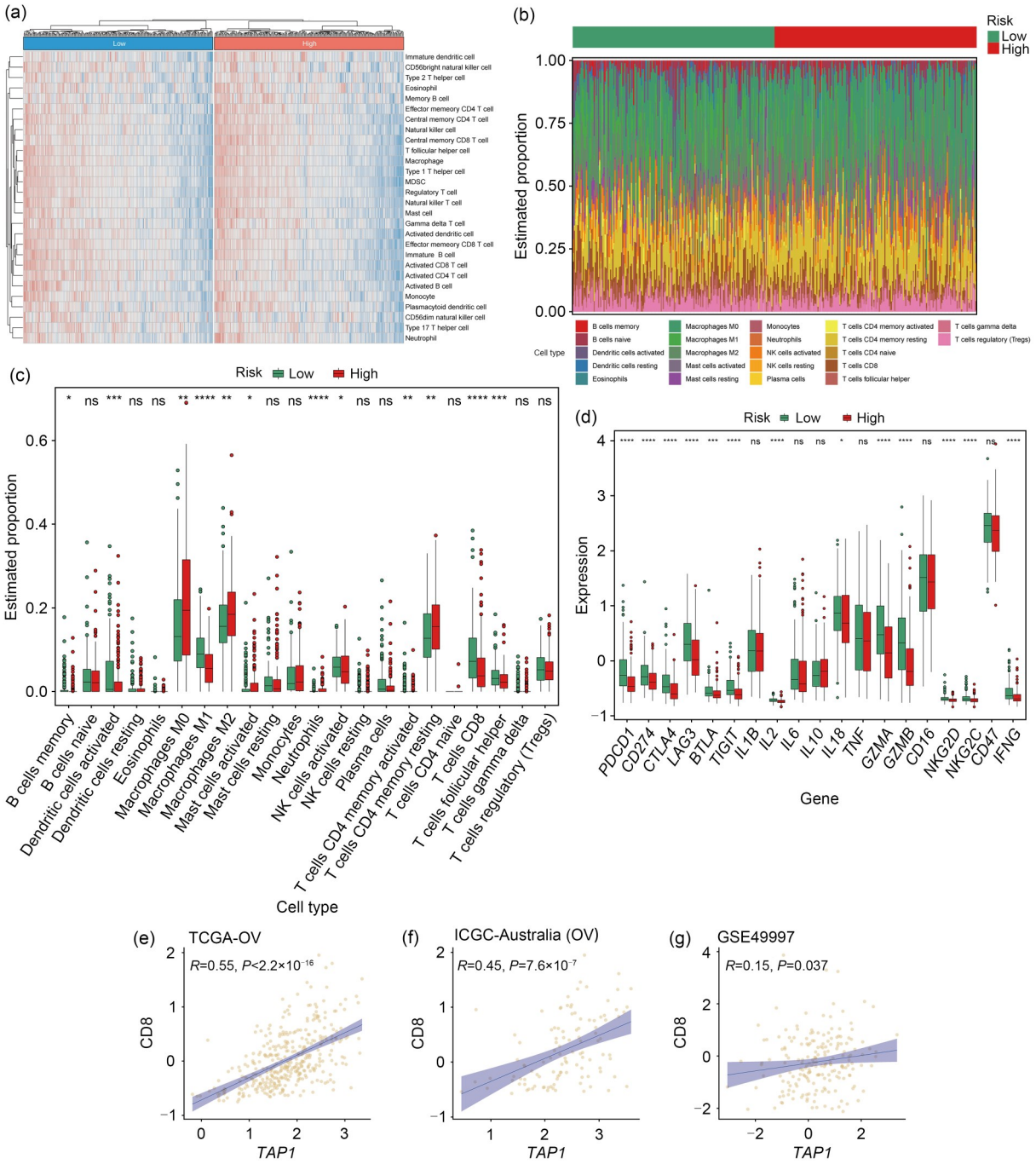

Fig. 6 Immune infiltrating profiles of the ER stress-related risk signature. (a) Heatmap of immune cell distribution in TCGA cohort according to the risk scores. (b, c) Comparison of the infiltration of 22 immune cells between low- and high-risk groups. (d) Comparison analysis of the immune molecules between low- and high-risk groups. Correlation analyses of *TAP1* expression and *CD8* in TCGA (e), ICGC (f), and GEO (g) cohorts. *R* represents regression coefficient. * *P*< 0.05, ** *P*<0.01, *** *P*<0.001, **** *P*<0.0001, ns: no significance. MDSC: myeloid-derived supperssor cell; ER: endoplasmic reticulum; TCGA: The Cancer Genome Atlas; ICGC: International Cancer Genome Consortium; GEO: Gene Expression Omnibus; OV: ovarian cancer; *CD8*: cluster of differentiation 8; *TAP1*: transporter 1 adenosine triphosphate (ATP)-binding cassette subfamily B member; NK: natural killer; *PDCD1*: programmed cell death 1; *CD*: cluster of differentiation; *CTLA4*: cytotoxic T-lymphocyte-associated antigen-4; *LAG3*: lymphocyte activation gene 3; *BTLA*: B- and T-lymphocyte attenuator; *TIGIT*: T cell immunoreceptor with Ig and ITIM domains; *IL*: interleukin; *TNF*: tumor necrosis factor; *GZMA*: granzyme A; *GZMB*: granzyme B; *NKG2D*: killer cell lectin-like receptor K1; *NKG2C*: killer cell lectin-like receptor C2; *IFNG*: interferon γ.

imply the infiltrating state of the anti-tumor component. Taken together, these results support the hypothesis that the ER stress-related risk signature might influence the disease progression by interacting with the immune microenvironment in OvCa.

3 Discussion

In this study, a seven-gene risk model related to ER stress was established for predicting the prognosis of OvCa patients. Particularly, we enrolled two datasets, with a total of 552 cases for the screening of prognostic genes, and applied the TCGA-OV cohort for risk model training based on sample size. Another two external datasets containing 304 cases were subsequently employed for validation. The K-M plots and nomograms showed a reliable characteristic, and the ROC curves of each cohort demonstrated the excellent robustness of our model. A close correlation between canonical ER stress pathway and our risk signature was further established. Finally, functional annotation and immune infiltration were performed to evaluate the profiles of the seven-gene panel in detail.

Although numerous studies have explored the influence of ER stress on OvCa in recent years (Barez et al., 2020; Lin et al., 2021; Zundell et al., 2021; Cheng et al., 2022), there is a surprising lack of reviews and bioinformatics based on this phenotype. We involved seven genes in our proposed model, and these genes could be divided into two groups: pernicious factors (*FOXO1*, *RB1*, *HSPA2*, *IGF2R*, and *TRPV4*) and protective factors (*ATP2A3* and *TAP1*).

FOXO1 protein, a TF encoded by *FOXO1*, has been reported to be critical in many cell processes, such as cell cycle modulation and oxidative stress regulation (Gao et al., 2012). According to Liu et al. (2020), the overexpression of FOXO1 was correlated with poor prognosis in OvCa. More recently, the role of FOXO proteins in cellular response to antitumor agents was reviewed by Beretta et al. (2019). Remarkably, many studies have depicted the chemo-resistant role of FOXO1 in the realm of OvCa research (Goto et al., 2008; Wang et al., 2015), while additional studies, as one performed by Tang et al. (2021), took a view to illustrate the relations between FOXO1-related pathway and ER stress; such studies are urgently needed. *RB1*, a tumor suppressor, was reported as commonly inactivated along with defective DNA repair in high-grade serous carcinoma (HGSC) (Patch et al., 2015; Shi et al., 2020). In line with our findings, Garsed et al. (2018) has shown that OvCa patients with *RB1* loss were associated with favorable outcomes. The underlying mechanism of this phenomenon may be attributable to dysfunction of mitochondria, which rendered vulnerabilities to stress conditions (Nicolay et al., 2015). Meanwhile, the detailed functions of *RB1* in OvCa related to ER stress remain to be uncovered.

Known as a stress-related gene, *HSPA2* belongs to the HSP70 subfamily of heat shock genes (Ścieglińska et al., 2008). Its overexpression is an ominous symbol associated with aggressive progression and poor prognosis in cancers, including esophageal carcinoma (Zhang et al., 2013), pancreatic adenocarcinoma (Zhai et al., 2021), lung cancer (Sojka et al., 2019), breast cancer (Yang et al., 2020), and epithelial OvCa (Zhao et al., 2021). Cao et al. (2019) aimed to reveal the relationship between *HSPA2* and ER stress, and found that *HSPA2* knockdown in lung adenocarcinoma cell lines upregulated the levels of IRE1α and PERK proteins, resulting in G1/S phase arrest via regulation of the extracellular-signal-regulated kinase 1/2 (Erk1/2) pathway. This critical role of HSPA2 contained in our risk model may evoke additional researches in this field.

IGF2R, also known as mannose-6-phosphate receptor (*M6P*), is generally considered as a tumor suppressor gene for its antagonistic activity to IGF1R signals (Leksa et al., 2017). A loss of heterozygosity (LOH) proximal to the *IGF2R*/*M6P* locus has been proved to be significantly correlated with the presence of disseminated tumor cells (DTCs) and shorter survival time in OvCa patients (Kuhlmann et al., 2011). Focusing on the detailed mechanism of trafficking, Wahba et al. (2018) found that the synergistic effect of chemo-immunotherapy was partly dependent on the shuttling of M6P to the OvCa cell surface. The reversed scenario that *IGF2R* serves as a hallmark of cancer has been recently demonstrated in a variety of cancers (Takeda et al., 2019; Zhang ZY et al., 2021). By disrupting the Golgi-to-lysosome transport of M6P-tagged cathepsins, the loss of *IGF2R* decreased lysosomal activity, with the dysfunction of both autophagy and mitophagy, resulting in the accumulation

of misfolded proteins and the production of ROS (Takeda et al., 2019), which may interact with ER stress-induced apoptosis.

TRPV4 is ubiquitously expressed in the central nervous system and mediates a lot of neuropathological processes (Wang et al., 2019; Liu et al., 2022). Meanwhile, in glioma, eminent work by Huang et al. (2021) showed that the TRPV4 level is positively correlated with both tumor grade and poor survival. Therein, the application of cannabidiol (CBD) induced lethal mitophagy through activating TRPV4 in human glioma cells. Later transcriptome analysis demonstrated that ER stress and the downstream of TRPV4 were involved in CBD-induced mitophagy in glioma cells (Huang et al., 2021). Meanwhile, TRPV4 was reported as highly expressed and associated with poor prognosis in OvCa patients. Further bioinformatics suggested that *TRPV4* might act as an oncogene through an immunosuppressive effect along with the underlying mechanism of resistance to platinum (Wang et al., 2021).

As a member of sarco/endoplasmic reticulum (SR/ER) Ca^{2+} ATPase pump (SERCA) family (Chemaly et al., 2018), ATP2A3 has recently been shown to be a potential target of salinomycin through the inhibition of Ca^{2+} release and the induction of ER stress in prostate cancer (Zhang et al., 2019). Coincidentally, thapsigargin (TG) was widely used as an irreversible inhibitor of the ER Ca^{2+} ATPase (Lei et al., 2015), which can synergize with many anti-cancer agents by triggering ER stress-related apoptosis in OvCa (Seo et al., 2016; Kim and Ko, 2021). However, *ATP2A3* in our risk model delivered a protective role for survival extension in accordance with the pro-apoptotic effect of *ATP2A3* defined by Chemaly et al. (2018). The seemingly debatable evidence might be attributed to the non-specific blocking effect of TG. Therefore, to further clarify the role of *ATP2A3* in OvCa, more specific agents or genetic tools targeting *ATP2A3* need to be applied.

Among the seven genes in our risk signature, *TAP1* is the most charming one that connects the immune profile with ER stress for its special role in antigen presentation. Closely related to the dysregulation of MHC-I antigen molecules, TAP1 deficiency was frequently reported as a signature of tumor immune escape (Sabapathy and Nam, 2008; Chow et al., 2021). A growing body of evidence derived from clinical data firmly supports our findings that lower expression of TAP1 might correlate with poor prognosis in OvCa patients (Millstein et al., 2020). In addition to the immune-related perspective, the fact that *TAP1* serves as a prognostic factor may be due to its mechanism of activation of ER stress according to Sabapathy and Nam (2008). Specifically, a study by Bartoszewski et al. (2011) uncovered that unfolded protein response (UPR)-activated XBP1 was involved in the upregulation of microRNA-346, which further interfered in the expression of TAP1 by targeting a 6-mer canonical seeding site.

Given the multiple characteristics of each gene, we analyzed the comprehensive effect of the risk signature to clarify the correlation with canonical ER stress pathways. Impressively, among the three cohorts, high-risk group showed a higher level of IRE1α/XBP1 and PERK arm activation, indicating a non-lethal role ER stress response that promotes cell adaptation to stress. By contrast, higher levels of *ATF4* and *CHOP* were found in the low-risk group, representing an unresolved status of ER homeostasis (Chen and Cubillos-Ruiz, 2021). Functional annotation further illustrated that the ER stress-related signature was closely associated with cellular response and senescence, Ca^{2+} transport, domain binding disorder, and T cell activation. In line with the findings above, immune infiltration analysis also demonstrated differences in anti-tumor efficiency between the two groups. For the innate immunity cluster, macrophage polarization was highlighted in the results. Consistently, Soto-Pantoja et al. (2017) reported that tumoral IRE1α inhibition could enhance macrophage-mediated cancer cell clearance, indicating M1 polarization. Meanwhile, ICD induced by unresolved ER stress may account for the higher level of activated DCs in the low-risk group as well as the activation of adaptive immunity (Kasikova et al., 2019). Surprisingly, the levels of immunosuppressive molecules such as programmed death-1 (PD-1) and cytotoxic T lymphocyte associated antigen-4 (CTLA4) were also raised in the low-risk group, suggesting an innovative approach to apply the immunotherapy in a certain population of OvCa. An eminent study unveiled that $CD8^+$ tumor-infiltrating lymphocytes influenced the OvCa patients' survival in a dose-response manner (Ovarian Tumor Tissue Analysis (OTTA) Consortium, 2017). Given the special role of TAP1 in pMHC-I formation, the correlation between *CD8* and

TAP1 expression was analyzed (Figs. 6e–6g), while further studies are required to clarify the subtle influence of ER stress on tumor-associated antigen processing. Struggling in an execrable TME, intratumoral immune cells are always confronted with various stress factors. Recent studies have ascertained that the activation of IRE1α/XBP1 arm in DCs and T cells could impair their anti-tumor functions in OvCa (Cubillos-Ruiz et al., 2015; Song et al., 2018), highlighting the prospect of targeting the ER stress-related pathway in intratumoral immune cells to enhance their anti-tumor capacity.

4 Conclusions

In summary, our work identified an ER stress-related risk signature, providing a novel annotation for OvCa prognosis prediction. The robustness of this signature was demonstrated by double validations. Moreover, it was confirmed that preferential arms of canonical ER stress pathways were involved in both low- and high-risk groups. The analyses of enrichment and immune infiltrating profiles produced significant findings for future research on the mechanisms between ER stress-related genes and anti-tumor immunity in OvCa.

Materials and methods

Detailed methods are provided in the electronic supplementary materials of this paper.

Acknowledgments

This work was supported by the Shanghai Shenkang Hospital Development Center's Shenkang Promotion of Clinical Skills and Clinical Innovation in Municipal Hospitals Three-Year Action Plan (No. 2020–2023), the Major Clinical Research Project (No. SHDC2020CR1048B), and the Pilot Construction Project of High-Level Universities in Shanghai (No. DGF501017-06), China.

Author contributions

Jiahang MO and Hua JIANG were responsible for the research design and conceptualization. Jiahang MO, Shunyi RUAN, and Baicai YANG collected the data. Shunyi RUAN and Yunfeng JIN performed the computational analyses. Jiahang MO and Baicai YANG drafted the manuscript. Yunfeng JIN and Xukai LUO revised the manuscript. Keyi LIU was consulted for molecular pathology of ovarian cancer. Hua JIANG supervised and supported this research. All authors have read and approved the final manuscript, and therefore, have full access to all the data in the study and take responsibility for the integrity and security of the data.

Compliance with ethics guidelines

Jiahang MO, Shunyi RUAN, Baicai YANG, Yunfeng JIN, Keyi LIU, Xukai LUO, and Hua JIANG declare that they have no conflict of interest.

This article does not contain any studies with human or animal subjects performed by any of the authors.

References

Andrews AM, Tennant MD, Thaxton JE, 2021. Stress relief for cancer immunotherapy: implications for the ER stress response in tumor immunity. *Cancer Immunol Immunother*, 70(5):1165-1175. https://doi.org/10.1007/s00262-020-02740-3

Barez SR, Atar AM, Aghaei M, 2020. Mechanism of inositol-requiring enzyme 1-alpha inhibition in endoplasmic reticulum stress and apoptosis in ovarian cancer cells. *J Cell Commun. Signal*, 14(4):403-415. https://doi.org/10.1007/s12079-020-00562-7

Bartoszewski R, Brewer JW, Rab A, et al., 2011. The unfolded protein response (UPR)-activated transcription factor X-box-binding protein 1 (XBP1) induces microRNA-346 expression that targets the human antigen peptide transporter 1 (TAP1) mRNA and governs immune regulatory genes. *J Biol Chem*, 286(48):41862-41870. https://doi.org/10.1074/jbc.M111.304956

Beretta GL, Corno C, Zaffaroni N, et al., 2019. Role of FoxO proteins in cellular response to antitumor agents. *Cancers (Basel)*, 11(1):90. https://doi.org/10.3390/cancers11010090

Cao LX, Yuan XS, Bao FC, et al., 2019. Downregulation of *HSPA2* inhibits proliferation via ERK1/2 pathway and endoplasmic reticular stress in lung adenocarcinoma. *Ann Transl Med*, 7(20):540. https://doi.org/10.21037/atm.2019.10.16

Chemaly ER, Troncone L, Lebeche D., 2018. SERCA control of cell death and survival. *Cell Calcium*, 69:46-61. https://doi.org/10.1016/j.ceca.2017.07.001

Chen X, Cubillos-Ruiz JR, 2021. Endoplasmic reticulum stress signals in the tumour and its microenvironment. *Nat Rev Cancer*, 21(2):71-88. https://doi.org/10.1038/s41568-020-00312-2

Cheng MY, Yu HM, Kong QH, et al., 2022. The mitochondrial PHB2/OMA1/DELE1 pathway cooperates with endoplasmic reticulum stress to facilitate the response to chemotherapeutics in ovarian cancer. *Int J Mol Sci*, 23(3):1320. https://doi.org/10.3390/ijms23031320

Chow K, Bedő J, Ryan A, et al., 2021. Ductal variant prostate carcinoma is associated with a significantly shorter metastasis-free survival. *Eur J Cancer*, 148:440-450. https://doi.org/10.1016/j.ejca.2020.12.030

Cubillos-Ruiz JR, Silberman PC, Rutkowski MR, et al., 2015. ER stress sensor XBP1 controls anti-tumor immunity by

disrupting dendritic cell homeostasis. *Cell*, 161(7):1527-1538.
https://doi.org/10.1016/j.cell.2015.05.025

Cubillos-Ruiz JR, Bettigole SE, Glimcher LH, 2016. Molecular pathways: immunosuppressive roles of IRE1α-XBP1 signaling in dendritic cells of the tumor microenvironment. *Clin Cancer Res*, 22(9):2121-2126.
https://doi.org/10.1158/1078-0432.CCR-15-1570

Fei HJ, Chen SC, Xu CM, 2021. Construction autophagy-related prognostic risk signature to facilitate survival prediction, individual treatment and biomarker excavation of epithelial ovarian cancer patients. *J Ovarian Res*, 14:41.
https://doi.org/10.1186/s13048-021-00791-3

Galluzzi L, Buqué A, Kepp O, et al., 2017. Immunogenic cell death in cancer and infectious disease. *Nat Rev Immunol*, 17(2):97-111.
https://doi.org/10.1038/nri.2016.107

Gao JC, Yang XJ, Yin P, et al., 2012. The involvement of FoxO in cell survival and chemosensitivity mediated by Mirk/Dyrk1B in ovarian cancer. *Int J Oncol*, 40(4):1203-1209.
https://doi.org/10.3892/ijo.2011.1293

Garsed DW, Alsop K, Fereday S, et al., 2018. Homologous recombination DNA repair pathway disruption and retinoblastoma protein loss are associated with exceptional survival in high-grade serous ovarian cancer. *Clin Cancer Res*, 24(3):569-580.
https://doi.org/10.1158/1078-0432.CCR-17-1621

González-Martín A, Pothuri B, Vergote I, et al., 2019. Niraparib in patients with newly diagnosed advanced ovarian cancer. *N Engl J Med*, 381(25):2391-2402.
https://doi.org/10.1056/NEJMoa1910962

Goto T, Takano M, Hirata J, et al., 2008. The involvement of FOXO1 in cytotoxic stress and drug-resistance induced by paclitaxel in ovarian cancers. *Br J Cancer*, 98(6):1068-1075.
https://doi.org/10.1038/sj.bjc.6604279

Han LY, Fletcher MS, Urbauer DL, et al., 2008. HLA class I antigen processing machinery component expression and intratumoral T-cell infiltrate as independent prognostic markers in ovarian carcinoma. *Clin Cancer Res*, 14(11):3372-3379.
https://doi.org/10.1158/1078-0432.CCR-07-4433

Harter P, Sehouli J, Vergote I, et al., 2021. Randomized trial of cytoreductive surgery for relapsed ovarian cancer. *N Engl J Med*, 385(23):2123-2131.
https://doi.org/10.1056/NEJMoa2103294

Huang TF, Xu TQ, Wang YF, et al., 2021. Cannabidiol inhibits human glioma by induction of lethal mitophagy through activating TRPV4. *Autophagy*, 17(11):3592-3606.
https://doi.org/10.1080/15548627.2021.1885203

Kasikova L, Hensler M, Truxova I, et al., 2019. Calreticulin exposure correlates with robust adaptive antitumor immunity and favorable prognosis in ovarian carcinoma patients. *J Immunother Cancer*, 7(1):312.
https://doi.org/10.1186/s40425-019-0781-z

Kim T, Ko SG, 2021. JI017, a complex herbal medication, induces apoptosis via the Nox4-PERK-CHOP axis in ovarian cancer cells. *Int J Mol Sci*, 22(22):12264.
https://doi.org/10.3390/ijms222212264

Kuhlmann JD, Schwarzenbach H, Otterbach F, et al., 2011. Loss of heterozygosity proximal to the *M6P/IGF2R* locus is predictive for the presence of disseminated tumor cells in the bone marrow of ovarian cancer patients before and after chemotherapy. *Genes Chromosomes Cancer*, 50(8):598-605.
https://doi.org/10.1002/gcc.20882

Lee JY, Ham J, Lim W, et al., 2020. Apomorphine facilitates loss of respiratory chain activity in human epithelial ovarian cancer and inhibits angiogenesis *in vivo*. *Free Radic Biol Med*, 154:95-104.
https://doi.org/10.1016/j.freeradbiomed.2020.05.001

Lei Y, Henderson BR, Emmanuel C, et al., 2015. Inhibition of ANKRD1 sensitizes human ovarian cancer cells to endoplasmic reticulum stress-induced apoptosis. *Oncogene*, 34(4):485-495.
https://doi.org/10.1038/onc.2013.566

Leksa V, Ilková A, Vičíková K, et al., 2017. Unravelling novel functions of the endosomal transporter mannose 6-phosphate/insulin-like growth factor receptor (CD222) in health and disease: an emerging regulator of the immune system. *Immunol Lett*, 190:194-200.
https://doi.org/10.1016/j.imlet.2017.08.011

Lheureux S, Braunstein M, Oza AM, 2019. Epithelial ovarian cancer: evolution of management in the era of precision medicine. *CA Cancer J Clin*, 69(4):280-304.
https://doi.org/10.3322/caac.21559

Lin JH, Liu H, Fukumoto T, et al., 2021. Targeting the IRE1α/XBP1s pathway suppresses CARM1-expressing ovarian cancer. *Nat Commun*, 12:5321.
https://doi.org/10.1038/s41467-021-25684-3

Liu LY, Yi JJ, Yuan JH, et al., 2020. FOXO1 overexpression is correlated with poor prognosis in epithelial ovarian cancer. *Cancer Biomark*, 28(1):1-8.
https://doi.org/10.3233/CBM-182119

Liu N, Bai LP, Lu ZP, et al., 2022. TRPV4 contributes to ER stress and inflammation: implications for Parkinson's disease. *J Neuroinflamm*, 19:26.
https://doi.org/10.1186/s12974-022-02382-5

Millstein J, Budden T, Goode EL, et al., 2020. Prognostic gene expression signature for high-grade serous ovarian cancer. *Ann Oncol*, 31(9):1240-1250.
https://doi.org/10.1016/j.annonc.2020.05.019

Nicolay BN, Danielian PS, Kottakis F, et al., 2015. Proteomic analysis of pRb loss highlights a signature of decreased mitochondrial oxidative phosphorylation. *Genes Dev*, 29(17):1875-1889.
https://doi.org/10.1101/gad.264127.115

Ovarian Tumor Tissue Analysis (OTTA) Consortium, 2017. Dose-response association of $CD8^+$ tumor-infiltrating lymphocytes and survival time in high-grade serous ovarian cancer. *JAMA Oncol*, 3(12):e173290.
https://doi.org/10.1001/jamaoncol.2017.3290

Patch AM, Christie EL, Etemadmoghadam D, et al., 2015. Whole-genome characterization of chemoresistant ovarian cancer. *Nature*, 521(7553):489-494.

https://doi.org/10.1038/nature14410

Poveda A, Floquet A, Ledermann JA, et al., 2021. Olaparib tablets as maintenance therapy in patients with platinum-sensitive relapsed ovarian cancer and a *BRCA1/2* mutation (SOLO2/ENGOT-Ov21): a final analysis of a double-blind, randomised, placebo-controlled, phase 3 trial. *Lancet Oncol*, 22(5):620-631.
https://doi.org/10.1016/s1470-2045(21)00073-5

Pujade-Lauraine E, Hilpert F, Weber B, et al., 2014. Bevacizumab combined with chemotherapy for platinum-resistant recurrent ovarian cancer: the AURELIA open-label randomized phase III trial. *J Clin Oncol*, 32(13):1302-1308.
https://doi.org/10.1200/JCO.2013.51.4489

Sabapathy K, Nam SY, 2008. Defective MHC class I antigen surface expression promotes cellular survival through elevated ER stress and modulation of p53 function. *Cell Death Differ*, 15(9):1364-1374.
https://doi.org/10.1038/cdd.2008.55

Ścieglińska D, Piglowski W, Mazurek A, et al., 2008. The HspA2 protein localizes in nucleoli and centrosomes of heat shocked cancer cells. *J Cell Biochem*, 104(6):2193-2206.
https://doi.org/10.1002/jcb.21778

Seo JA, Kim B, Dhanasekaran DN, et al., 2016. Curcumin induces apoptosis by inhibiting sarco/endoplasmic reticulum Ca^{2+} ATPase activity in ovarian cancer cells. *Cancer Lett*, 371(1):30-37.
https://doi.org/10.1016/j.canlet.2015.11.021

Shi MX, Whorton AE, Sekulovski N, et al., 2020. Inactivation of TRP53, PTEN, RB1, and/or CDH1 in the ovarian surface epithelium induces ovarian cancer transformation and metastasis. *Biol Reprod*, 102(5):1055-1064.
https://doi.org/10.1093/biolre/ioaa008

Sojka DR, Gogler-Pigłowska A, Vydra N, et al., 2019. Functional redundancy of HSPA1, HSPA2 and other HSPA proteins in non-small cell lung carcinoma (NSCLC); an implication for NSCLC treatment. *Sci Rep*, 9:14394.
https://doi.org/10.1038/s41598-019-50840-7

Song M, Sandoval TA, Chae CS, et al., 2018. IRE1α-XBP1 controls T cell function in ovarian cancer by regulating mitochondrial activity. *Nature*, 562(7727):423-428.
https://doi.org/10.1038/s41586-018-0597-x

Soto-Pantoja DR, Wilson AS, Clear KYJ, et al., 2017. Unfolded protein response signaling impacts macrophage polarity to modulate breast cancer cell clearance and melanoma immune checkpoint therapy responsiveness. *Oncotarget*, 8(46):80545-80559.
https://doi.org/10.18632/oncotarget.19849

Sung H, Ferlay J, Siegel RL, et al., 2021. Global Cancer Statistics 2020: GLOBOCAN Estimates of Incidence and Mortality Worldwide for 36 Cancers in 185 Countries. *CA Cancer J Clin*, 71(3):209-249.
https://doi.org/10.3322/caac.21660

Takeda T, Komatsu M, Chiwaki F, et al., 2019. Upregulation of IGF2R evades lysosomal dysfunction-induced apoptosis of cervical cancer cells via transport of cathepsins. *Cell Death Dis*, 10(12):876.
https://doi.org/10.1038/s41419-019-2117-9

Tang YB, Chen J, Li JQ, et al., 2021. Pristimerin synergistically sensitizes conditionally reprogrammed patient derived-primary hepatocellular carcinoma cells to sorafenib through endoplasmic reticulum stress and ROS generation by modulating Akt/FoxO1/$p27^{kip1}$ signaling pathway. *Phytomedicine*, 86:153563.
https://doi.org/10.1016/j.phymed.2021.153563

Tian WJ, Lei NJ, Zhou JY, et al., 2022. Extracellular vesicles in ovarian cancer chemoresistance, metastasis, and immune evasion. *Cell Death Dis*, 13:64.
https://doi.org/10.1038/s41419-022-04510-8

Wahba J, Natoli M, Whilding LM, et al., 2018. Chemotherapy-induced apoptosis, autophagy and cell cycle arrest are key drivers of synergy in chemo-immunotherapy of epithelial ovarian cancer. *Cancer Immunol Immunother*, 67(11):1753-1765.
https://doi.org/10.1007/s00262-018-2199-8

Wang JL, Yang H, Li WJ, et al., 2015. Thioredoxin 1 upregulates FOXO1 transcriptional activity in drug resistance in ovarian cancer cells. *Biochim Biophys Acta*, 1852(3):395-405.
https://doi.org/10.1016/j.bbadis.2014.12.002

Wang K, Feng XJ, Zheng LZ, et al., 2021. TRPV4 is a prognostic biomarker that correlates with the immunosuppressive microenvironment and chemoresistance of anticancer drugs. *Front Mol Biosci*, 8:690500.
https://doi.org/10.3389/fmolb.2021.690500

Wang ZQ, Zhou L, An D, et al., 2019. TRPV4-induced inflammatory response is involved in neuronal death in pilocarpine model of temporal lobe epilepsy in mice. *Cell Death Dis*, 10(6):386.
https://doi.org/10.1038/s41419-019-1612-3

Yang YL, Zhang Y, Li DD, et al., 2020. RNF144A functions as a tumor suppressor in breast cancer through ubiquitin ligase activity-dependent regulation of stability and oncogenic functions of HSPA2. *Cell Death Differ*, 27(3):1105-1118.
https://doi.org/10.1038/s41418-019-0400-z

Ye Y, Dai QJ, Li SH, et al., 2021. A novel defined risk signature of the ferroptosis-related genes for predicting the prognosis of ovarian cancer. *Front Mol Biosci*, 8:645845.
https://doi.org/10.3389/fmolb.2021.645845

Zhai LL, Qiao PP, Sun YS, et al., 2021. Upregulated HSPA2 predicts early relapse of pancreatic cancer after surgery. *Gland Surg*, 10(7):2140-2149.
https://doi.org/10.21037/gs-21-262

Zhang B, Nie XC, Miao XX, et al., 2021. Development and verification of an immune-related gene pairs prognostic signature in ovarian cancer. *J Cell Mol Med*, 25(6):2918-2930.
https://doi.org/10.1111/jcmm.16327

Zhang H, Chen W, Duan CJ, et al., 2013. Overexpression of HSPA2 is correlated with poor prognosis in esophageal squamous cell carcinoma. *World J Surg Oncol*, 11:141.
https://doi.org/10.1186/1477-7819-11-141

Zhang YQ, Wang YN, Zhao GY, et al., 2022. FOXK2 promotes ovarian cancer stemness by regulating the unfolded protein response pathway. *J Clin Invest*, 132(10):e151591.
https://doi.org/10.1172/JCI151591

Zhang YS, Li F, Liu LG, et al., 2019. Salinomycin triggers endoplasmic reticulum stress through ATP2A3 upregulation in PC-3 cells. *BMC Cancer*, 19:381. https://doi.org/10.1186/s12885-019-5590-8

Zhang ZY, Mou ZZ, Xu CY, et al., 2021. Autophagy-associated circular RNA hsa_circ_0007813 modulates human bladder cancer progression via hsa-miR-361-3p/IGF2R regulation. *Cell Death Dis*, 12(8):778. https://doi.org/10.1038/s41419-021-04053-4

Zhao LB, Ma SJ, Wang LCH, et al., 2021. A polygenic methylation prediction model associated with response to chemotherapy in epithelial ovarian cancer. *Mol Ther Oncolytics*, 20:545-555. https://doi.org/10.1016/j.omto.2021.02.012

Zundell JA, Fukumoto T, Lin JH, et al., 2021. Targeting the IRE1α/XBP1 endoplasmic reticulum stress response pathway in *ARID1A*-mutant ovarian cancers. *Cancer Res*, 81(20):5325-5335. https://doi.org/10.1158/0008-5472.CAN-21-1545

Supplementary information

Materials and methods; Tables S1 and S2; Figs. S1–S3